catalysts

MDPI

Article

New Magnetically Assembled Electrode Consisting of Magnetic Activated Carbon Particles and Ti/Sb-SnO_2 for a More Flexible and Cost-Effective Electrochemical Oxidation Wastewater Treatment

Fanxi Zhang [1], Dan Shao [1,*], Changan Yang [1], Hao Xu [2,*], Jin Yang [1], Lei Feng [1], Sizhe Wang [1], Yong Li [1], Xiaohua Jia [1] and Haojie Song [1,*]

[1] School of Materials Science and Engineering, Shaanxi Key Laboratory of Green Preparation and Functionalization for Inorganic Materials, Shaanxi University of Science & Technology, Xi'an 710021, China
[2] Department of Environmental Engineering, Xi'an Jiaotong University, Xi'an 710049, China
* Correspondence: shaodan@sust.edu.cn (D.S.); xuhao@mail.xjtu.edu.cn (H.X.); songhaojie@sust.edu.cn (H.S.)

Abstract: Magnetic activated carbon particles (Fe_3O_4/active carbon composites) as auxiliary electrodes (AEs) were fixed on the surface of Ti/Sb-SnO_2 foil by a NdFeB magnet to form a new magnetically assembled electrode (MAE). Characterizations including cyclic voltammetry, Tafel analysis, and electrochemical impedance spectroscopy were carried out. The electrochemical oxidation performances of the new MAE towards different simulated wastewaters (azo dye acid red G, phenol, and lignosulfonate) were also studied. Series of the electrochemical properties of MAE were found to be varied with the loading amounts of AEs. The electrochemical area as well as the number of active sites increased significantly with the AEs loading, and the charge transfer was also facilitated by these AEs. Target pollutants' removal of all simulated wastewaters were found to be enhanced when loading appropriate amounts of AEs. The accumulation of intermediate products was also determined by the AEs loading amount. This new MAE may provide a landscape of a more cost-effective and flexible electrochemical oxidation wastewater treatment (EOWT).

Keywords: anode; metal oxide; electrolysis; refractory pollutant; carbon

check for updates

Citation: Zhang, F.; Shao, D.; Yang, C.; Xu, H.; Yang, J.; Feng, L.; Wang, S.; Li, Y.; Jia, X.; Song, H. New Magnetically Assembled Electrode Consisting of Magnetic Activated Carbon Particles and Ti/Sb-SnO_2 for a More Flexible and Cost-Effective Electrochemical Oxidation Wastewater Treatment. *Catalysts* **2023**, *13*, 7. https://doi.org/10.3390/catal13010007

Academic Editor: Enric Brillas

Received: 19 November 2022
Revised: 14 December 2022
Accepted: 18 December 2022
Published: 22 December 2022

Copyright: © 2022 by the authors. Licensee MDPI, Basel, Switzerland. This article is an open access article distributed under the terms and conditions of the Creative Commons Attribution (CC BY) license (https://creativecommons.org/licenses/by/4.0/).

1. Introduction

Industrial organic wastewaters are difficult to be simply treated by conventional biological, physical, and chemical methods due to their complex composition, recalcitrance, and high toxicity [1,2]. Electrochemical oxidation wastewater treatment (EOWT), a cutting-edge advanced oxidation technology, is an effective, adaptable, straightforward, and environmentally friendly approach to treat such refractory wastewaters using clean electrons [3,4].

The anode has a direct impact on the effectiveness and selectivity of EOWT, so choosing an appropriate anode material with as many active sites as possible is crucial in a specific case [5,6]. However, the traditional two-dimensional electrode has insufficient area to provide adequate amounts of active sites, and the advanced three-dimensional electrode has high investment cost and poor recyclability [7,8]. In addition, these anodes are non-variable, which could not provide sustainably high efficiency over a broad range of inlet wastewaters. In view of this, a variable electrode format is needed to avoid electrode updating or system shutting down as possible.

In recent years, we proposed a novel electrode architecture consisting of a two-dimensional titanium-based metal oxide electrode (main electrodes, ME), a number of magnetic catalyst particles with Fe_3O_4 cores and coatings (auxiliary electrodes, AEs), and a permanent magnet (see Scheme 1). The AEs are fixed on the ME surface by magnetic force provided by the permanent magnet. This adjustable and modular electrode format is

named the magnetically assembled electrode (MAE) [9,10]. By varying the magnetic force, a flexible and in situ electrode surface modification could be realized. Furthermore, the physically combined electrode has excellent maintainability and recyclability. The synergistic effect of the ME and AEs improves the electrode activity, and the timely replacement of the AEs can achieve flexible tunability and a long lifetime.

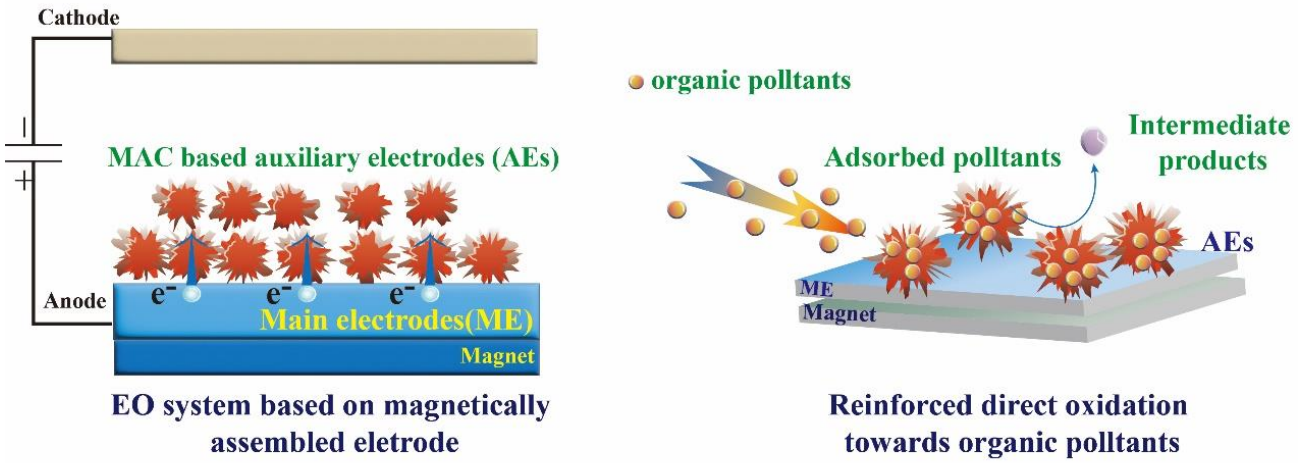

Scheme 1. Structure of the MAE used in this study and the role provided by the MAC in the MAE.

In our earlier research, nearly all kinds of AEs were coated by metal oxides (e.g., Sb-SnO_2 and Pb_3O_4) or conducting polymers (e.g., polyaniline), and the adopted ME coatings were typical dimensional stable anode (DSA) coatings (e.g., PbO_2, Sb-SnO_2, RuO_2-IrO_2-TiO_2, and IrO_2-Ta_2O_5) or others (Pt, graphite) [9–15]. We discovered that increasing the loading amount of AEs can elevate series of electrochemical properties of MAE. In brief, the AEs provide massive active sites, but which are mainly less accessible active sites. Good mass transfer and high current efficiency of pollutant degradation could benefit from these additional active sites [11–15]. Unfortunately, the conductivity of these AEs is insufficient, which may lead to the uneven distribution of anodic potential throughout the AEs layers and the insufficient polarization degree of the outer layers. Therefore, excessive AEs loading is not advised. Fortunately, we also found that ME with good oxygen evolution reaction (OER) activity has an activating effect on AEs and can mitigate the above problems to some extent [13,14].

In this study, we developed a kind of magnetic activated carbon particles (referred to as MAC, i.e., Fe_3O_4/active carbon composites) with stable physicochemical properties, good electrical conductivity, and well-developed pores [7,8]. These MAC particles were expected to further release the potential of MAE for faster electron transfer and more electrochemical area. Ti/Sb-SnO_2 with poor OER activity was used as the ME to reflect the contribution of the new AEs. The effects of the AEs loading amount on the structure–activity of the MAE were thoroughly assessed through material characterizations and electrochemical characterizations. The effects of the AEs loading amount on the EOWT efficiency and selectivity were disclosed by the degradation treatments of azo dye acid red G (ARG), phenol (C_6H_5OH), and sodium lignosulphonate (lignin). This study also aims to enrich the material system of MAE, complete the structure—activity relationship theory of MAE, and provide additional theoretical basis and technical assistance to the application of EOWT towards actual organic wastewaters.

2. Results and Discussion

2.1. Material Characterization

The SEM image (×500) of the ME is shown in Figure 1a. A thick layer of Sb-SnO_2 coating effectively covered most of the titanium substrate and inhibited possible substrate passivation during electrolysis. However, the thermal decomposition process inevitably

causes the crack coating morphology. The XRD patterns of the ME and AEs are shown in Figure 1b. Five diffraction peaks of the ME at 2θ degrees of 26.6°, 33.9°, 37.9°, 51.8°, and 54.8° correspond to (110), (101), (200), (211), and (220) facets of tetragonal rutile phase SnO_2, respectively, according to the standard card (JCPDS 41-1445). A diffraction peak of Ti substrate is also identified due to the thin coating and high penetrability of X-ray. In the high depth of field micrograph on the macro level, the surface of ME is relatively flat, and the coating is relatively uniform (Figure 1c).

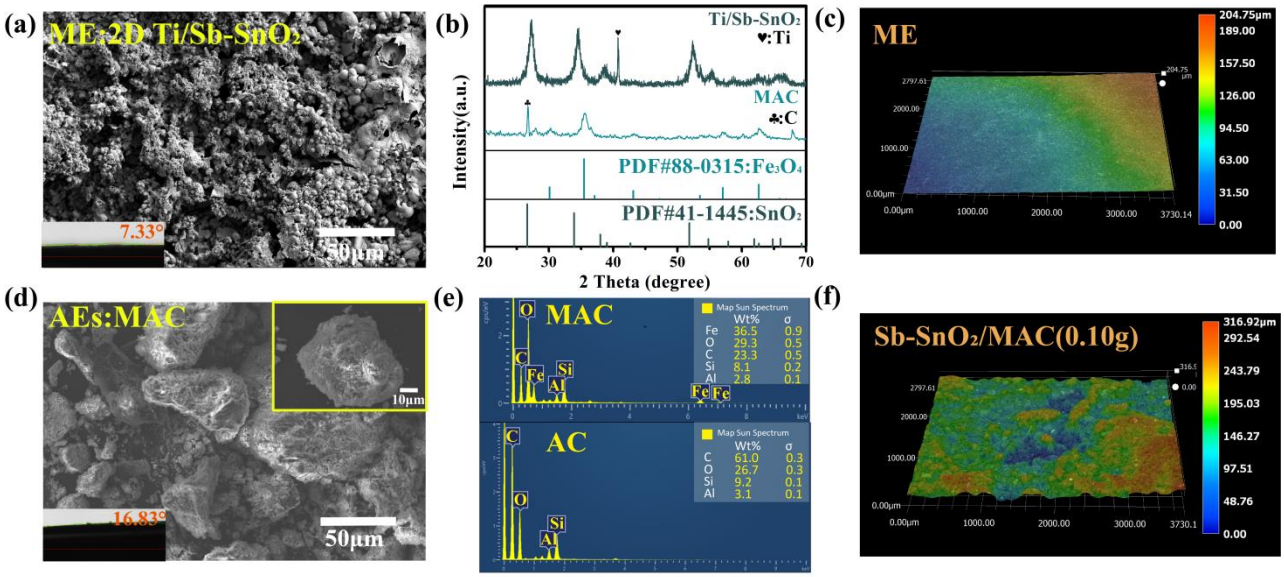

Figure 1. Material characterization results: (**a**) SEM image (×500) of ME (inset: water contact angle); (**b**) XRD of ME and AEs; (**c**) High depth of field micrograph of ME; (**d**) SEM image of (×500) of MAC (insets: SEM image of MAC (×1000) and water contact angle (very low angle, the numbers are just for reference)); (**e**) EDS element mappings of MAC and AC; (**f**) High depth of field micrograph of Sb-SnO_2/MAC(0.10 g).

The SEM image (×500, ×1000) of the MAC AEs are shown in Figure 1d, manifesting their rough surface. XRD result shows that these AEs contains Fe_3O_4 grains, demonstrating Fe_3O_4 is successfully deposited on the AC, making it magnetic (Figure 1b). EDS mappings of the AEs (Figure 1e) also verify that the MAC AEs are successfully prepared, which contain 36.5% of Fe, 29.3% of O, 23.3% of C, 8.1% of Si, and 2.8% of Al comparing with the original AC (Figure 1e, atom %).

The high depth of field micrograph of the Sb-SnO_2/MAC(0.10 g) is shown in Figure 1f. Loading AEs modifies the macroscopic surface roughness of the electrode and also changed the porosity and actual area of the electrode. It is also clear that the AEs are successfully fixed on the ME surface by the magnetic force. The hydrophilicity of the electrode remains well even when after loading the AEs (insets in Figure 1a,d).

2.2. Electrochemical Characterization

The narrow CV curves (0–0.3 V (vs. SCE)) for the ME (2D Ti/Sb-SnO_2), Sb-SnO_2/MAC (0.01 g), and Sb-SnO_2/MAC(0.10 g) obtained at 0.05 $V \cdot s^{-1}$ of potential scan rate are displayed in Figure 2a. The full view of narrow CV curves of all electrodes under different potential scan rates is illustrated in the Supporting Information (Figure S1). It can be seen that both the current density and the curve area significantly increase with the AEs (Figure 2a). A linear fit of the current density values and integral areas obtained from the narrow CV curves (Figure S1) in the non-Faraday region under different potential scan rates were used to determine the double-layer capacitance (C_{dl}) and voltammetric charges (q*), respectively (details are described in the Supporting Information Section and illustrated in Scheme S1). The q* could be categorized as the total voltammetric charge (q_T),

outer voltammetric charge (q_o), and inner voltammetric charge (q_i), which correspond to the total number of active sites, easily accessible external active sites, and less accessible internal active sites, respectively. Figure 2b demonstrates that increasing AEs' loading amount alters the electrode's structure, increasing the electrochemical area. For example, Sb-SnO_2/MAC(0.10 g) increases the C_{dl} by ~50% compared with the 2D Ti/Sb-SnO_2 electrode. Figure 2c shows adding 0.10 g·cm^{-2} of MAC can increase the number of q_i by 78.5%. The significant increases of C_{dl} and q* could benefit to the mass transfer and adsorption of pollutants, and the AEs can provide more additional catalytic active sites for the electrocatalytic reaction, leading to faster kinetics [11–15]. Therefore, the electrode's direct electron transfer (DET) capability may be improved by the addition of MAC AEs. Figure S2 shows the obvious variations of q* value with the addition of different pollutants, manifesting the effect of adsorbed pollutant on the charge–discharge process of the electrode, especially for MAEs.

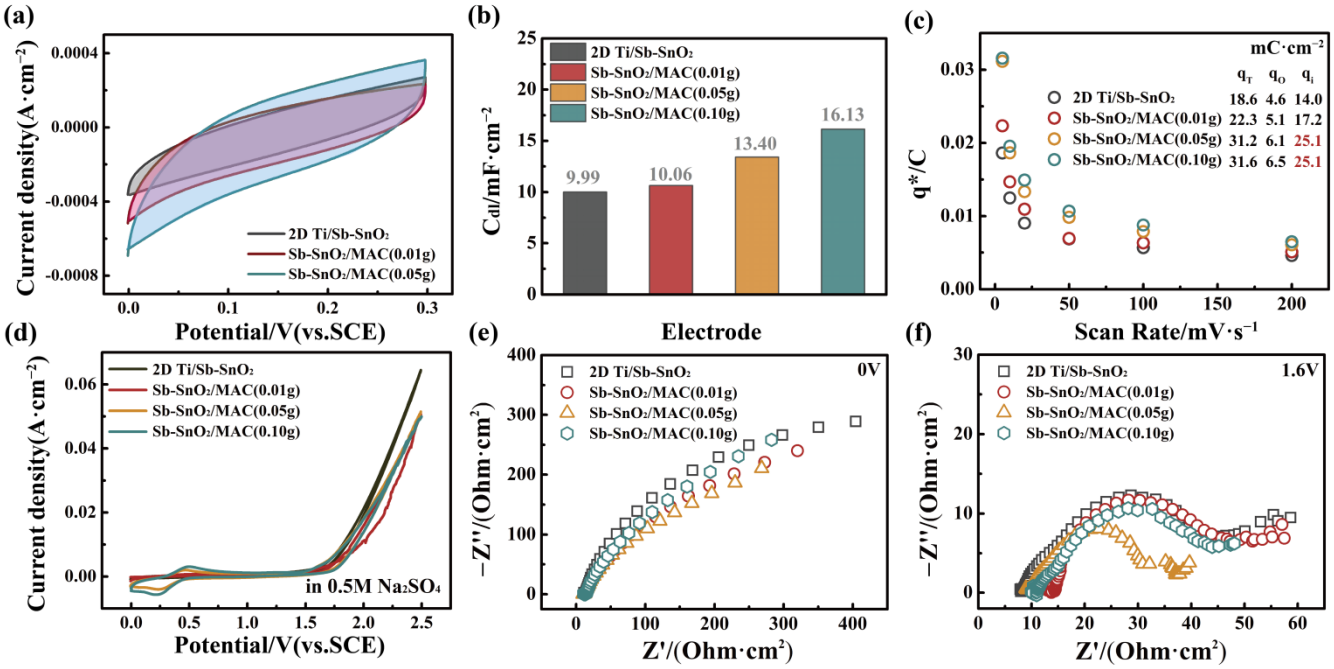

Figure 2. Electrochemical characterization results (in 0.5 M Na_2SO_4 solution): (**a**) Narrow CV curves of 2D Ti/Sb-SnO_2, Sb-SnO_2/MAC(0.01 g), and Sb-SnO_2/MAC(0.10 g) under potential scan rate of 0.005 V·s^{-1}; (**b**) C_{dl} values; (**c**) Voltammetric charges caculated from the narrow CV curves; (**d**) Normal CV curves (0–2.5 V vs. SCE, potential scan rate: 0.01 V·s^{-1}); (**e**) Nyquist plots (equilibrium potential of 0 V (vs. SCE)); (**f**) Nyquist plots (equilibrium potential of 1.6 V (vs. SCE)).

Normal CV curves (0–2.5 V (vs. SCE)) shown in Figure 2d and LSV curves shown in Figure S3 (Supporting Information) could further manifest the effect of MAC AEs on the electrode's electrochemical behaviors. Two-dimensional Ti/Sb-SnO_2 has the onset oxygen evolution potential (OEP) of ~1.80 V (vs. SCE). When AEs are present, the electrode's OEP rises slightly and the response current value in oxygen evolution reaction (OER) zone significantly reduces. Two new redox peaks appeared on MAEs' normal CV curves at ~0.5 V and 0.25 V (vs. SCE), respectively, which may be attributed to the redox of carbon and hydroxyl carbon. This phenomenon indicates that the physically bonded MAC AEs really take part in the electrochemical processes, introducing their own redox reactions before the OER, increasing the electrode's charging/discharging capacity, and inhibiting the OER activity of the electrode.

The enhanced electrode conductivity could also be reflected by the Nyquist plots of MAE in Figure 2e,f. The activated carbon particles could offer excellent conductivity and well-developed pore structure [7,8,16,17], which are beneficial to charge transfer and mass

transfer. However, only loading appropriate amount of AEs (i.e., for Sb-SnO_2/MAC(0.05 g)) would achieve the best result.

When three kinds of pollutants are added, the variations of normal CV curves (0–2.5 V (vs. SCE)) shown in Figure 3 could furtherly verify the enhanced DET process as well as the direct oxidation of pollutants introduced by the MAC AEs. The current response in the OER region is significantly decreased, and no current pollutant oxidation peak is found for 2D Ti/Sb-SnO_2 (Figure 3a,c). As a contrast, the current response in the OER region is nearly unchanged, and several pollutant oxidation peaks (or obvious current enhancement) are found between 1.2 V to 1.5 V (vs. SCE) for Sb-SnO_2/MAC(0.10 g) (Figure 3b,d). This result could furtherly verify that prior to the occurrence of OER (low applied potential), the three organic pollutants can undergo direct oxidation or DET process thanks to the introduction of MAC AEs. In addition, the electron transfer or mass transfer rate is faster on MAE than on 2D Ti/Sb-SnO_2 (see results in Figure 2), thus the pollutant oxidation on MAE could compensate the OER current decrease when the applied potential is high.

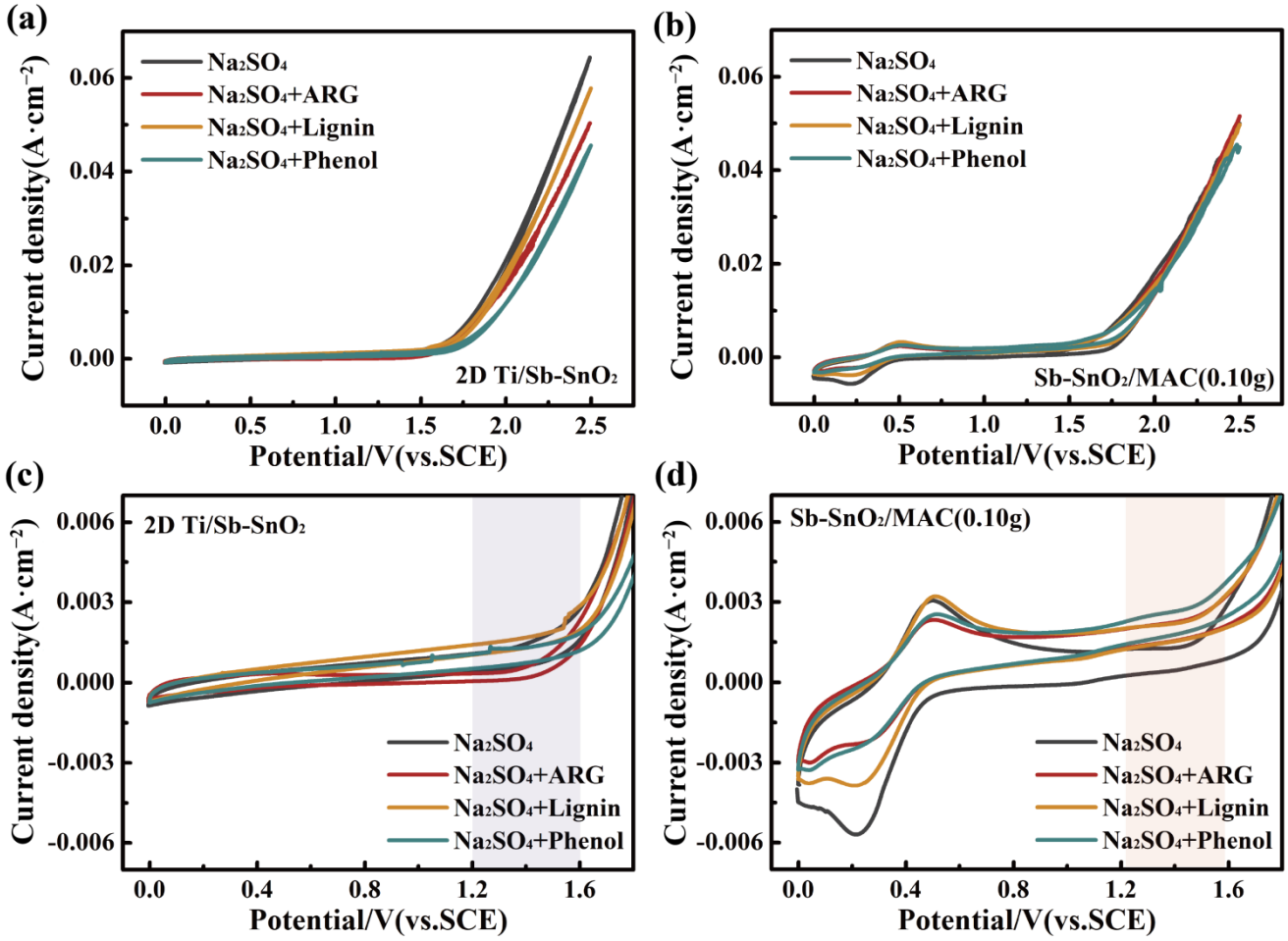

Figure 3. Normal CV curves of the electrodes (0–2.5 V (vs. SCE); scan rate: 0.01 $V \cdot s^{-1}$) in 0.5 M Na_2SO_4 solution and 0.5 M Na_2SO_4 solution with 2000 ppm of ARG, lignin or phenol: (**a**) 2D Ti/Sb-SnO_2; (**b**) Sb-SnO_2/MAC(0.10 g); (**c**) Partial enlarged view of 2D Ti/Sb-SnO_2; (**d**) Partial enlarged view of Sb-SnO_2/MAC(0.10 g).

2.3. Pollutant Degradation

2.3.1. Degradation of ARG

The destroying of the azo linkage of ARG is what we focus on due to its toxicity and character of chromophore. Direct oxidation or the DET process is as efficient as the hydroxyl radicals (indirect oxidation) in breaking the azo linkage [18,19]. Therefore, the

current densities of both 2 mA·cm^{-2} and 20 mA·cm^{-2} were selected as comparison. It is known from the previous normal CV or LSV curves that only 2 mA·cm^{-2} of current density benefits to direct oxidation (or DET process) while 20 mA·cm^{-2} has reinforced indirect oxidation effect [5,16]. Another reason for choosing these two current densities is that the mass transfer requirements are different under these two conditions.

From Figure 4 it can be found that the 15 min of pre-adsorption process has little effect on ARG removal, indicating MAC has insufficient absorption ability comparing with the traditional AC we anticipated. As seen from Figure 4a, and at low current density (2 mA·cm^{-2}), the EOWT basically follows the zero-order reaction kinetics (kinetics control). Sb-SnO_2/MAC(0.01 g) and Sb-SnO_2/MAC(0.05 g) do not show their superiority under this condition due to low anodic potential. However, Sb-SnO_2/MAC(0.10 g) show 100% higher efficiency than the 2D Ti/Sb-SnO_2 electrode. At high current density (e.g., 20 mA·cm^{-2}, Figure 4b) corresponding to high anodic potential, the kinetics control turns to mass transfer control. All electrodes show improved ARG degradation efficiencies, especially for the three MAEs. For example, Sb-SnO_2/MAC(0.10g) could achieve ARG removal efficiency from ~50% (2 mA·cm^{-2}) to above 90% (20 mA·cm^{-2}) after 3 h treatment, while 2D Ti/Sb-SnO_2 only has minor enhancement.

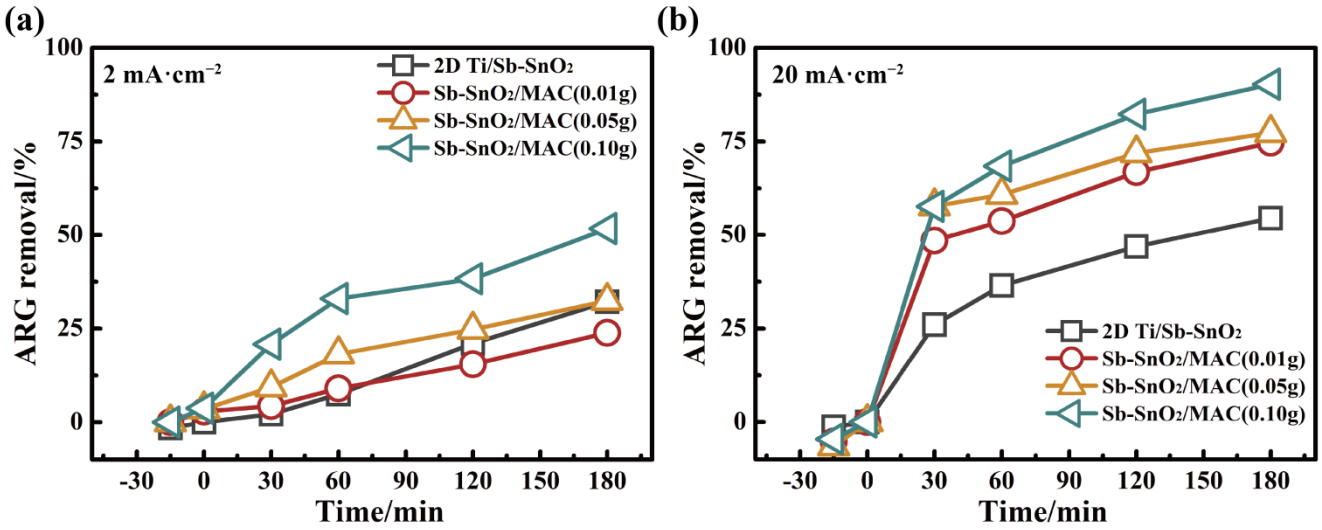

Figure 4. Degradation results of ARG (initial ARG concentration of 200 ppm, anode area of 9 cm^2, solution volume of 250 mL, 125 ppm of Na_2SO_4 as supporting electrolyte, room temperature): (**a**) ARG removal percentage versus time under low current density (2 mA·cm^{-2}); (**b**) ARG removal percentage versus time under high current density (20 mA·cm^{-2}).

The above results reflect the MAC's functions in improving electrode's electrochemical properties (Figures 2 and 3). The above results also demonstrate the superiorities of the MAEs in terms of reinforced direction oxidation (or DET) and improved mass transfer. More importantly, more electrochemical area or active sites brought by MAC AEs also lower the real current density significantly (under galvanostatic mode), which would further inhibit OER side reaction and benefit the DET process. The variations of UV-vis spectra, total dissolved solids (TDS), and pH value during ARG treatment are also placed in the Supporting Information for reference (Figure S5).

2.3.2. Degradation of Phenol

The structure of phenol requires a higher degradation ability of the electrode (ring opening). Phenol has a strong absorption peak at 270 nm in the UV region, which can reflect the phenol content (Figure S6, Supporting Information). From Figure S6 it can be seen that no matter whether under lower or higher current density, the 2D Ti/Sb-SnO_2 electrode could not effectively handle this pollutant. The addition of the MAC AEs could make the

solution's color deepen versus electrolysis time (from colorless to tea-brown and finally becoming turbid). A higher AEs loading amount would cause partial UV-vis adsorption peak shift phenomena under higher current density. These optical or spectral phenomena may reveal the effective oxidation of phenol to polymers or other intermediate products by MAEs.

Phenol adsorption is more negligible on these MAEs comparing with ARG (not shown here). After 3 h degradation of 100 ppm phenol, Figure 5 displays the mass-to-charge ratio (m/z) versus GC retention time of the organics present in the samples using bubble plots. In addition, the content of phenol and its intermediate degradation products can be visually reflected by the bubble area (corresponding to the GC peak area; two identified substances (m/z: 218, m/z: 206, which might be bimolecular polymers) and were the main intermediate products. The degradation effects of anodes varied greatly. In summary, loading more MAC AEs leads to more effective phenol degradation and less intermediate products accumulation, which is consistent with the electrochemical characterization results. The most effective electrode for removing phenol is Sb-SnO_2/MAC(0.10 g), with phenol removal efficiency of almost 100% and with the fewest accumulation of intermediate products. Sb-SnO_2/MAC(0.05 g) has phenol removal efficiency of ~80%. However, the performance of Sb-SnO_2/MAC(0.01 g) and 2D Ti/Sb-SnO_2 are similarly poor (only ~50% phenol removal). The above result indicates that the reinforced direct oxidation (or DET) caused by sufficient MAC AEs loading amount is necessary for phenol removal and intermediate products (e.g., polymers) elimination.

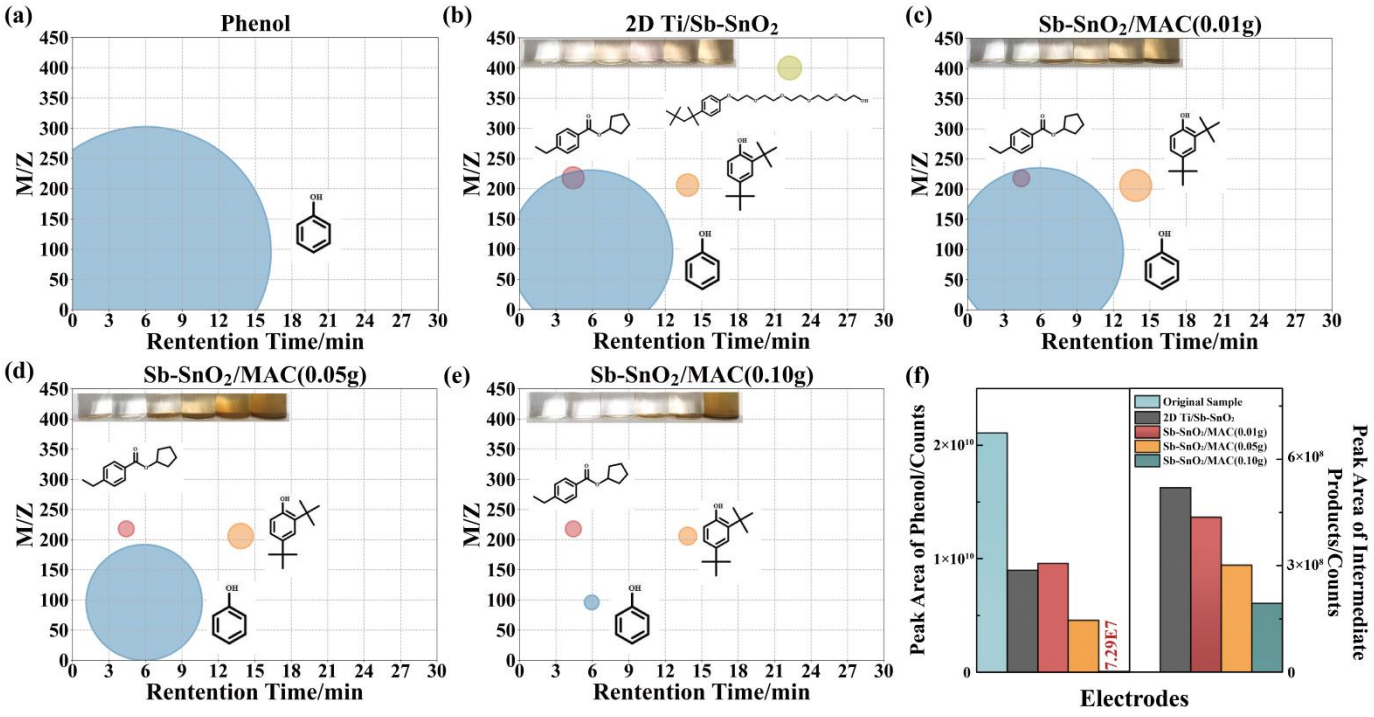

Figure 5. Phenol degradation results under current density of 20 mA·cm^{-2} (initial phenol concentration of 100 ppm, anode area of 9 cm^2, solution volume of 250 mL, supporting electrolyte of 125 ppm of Na_2SO_4, room temperature) before and after 3 h electrolysis: (**a**–**e**) Bubble diagrams of phenol or intermediate products according to their GC peak area ((**a**) Original sample of phenol; (**b**) 2D Ti/Sb-SnO_2 (inset: photos of the solution samples); (**c**) Sb-SnO_2/MAC(0.01 g) (inset: photos of the solution samples); (**d**) Sb-SnO_2/MAC(0.05 g) (inset: photos of the solution samples); (**e**) Sb-SnO_2/MAC(0.10 g) (inset: photos of the solution samples)); (**f**) Accumulative GC peak area columns of phenol and intermediate products.

2.3.3. Degradation of Lignin

Lignin is a series of three-dimensional macromolecules containing various functional groups such as methoxy, carbonyl, aldehyde, etc. It is a more complex organic compound than ARG and phenol, and this organic pollutant is most common in paper wastewater [20,21]. The advisable and cost-effective way to treat lignin wastewater is just to enhance its biodegradability. That is, breaking the linkage bonds (C-C and C-O-C bonds) between the lignin structural units while also avoiding over-oxidation so as to obtain useful small molecular resources such as alcohols, acids, and phenolic derivatives. We found MAE is still applicable to this complex and refractory organic wastewater (Figures 6 and S7). For 2D Ti/Sb-SnO_2, under two different current densities, the UV-vis spectra versus time were nearly unchanged, and the changes in pH and TDS were relatively inconspicuous, suggesting 2D Ti/Sb-SnO_2 could not effectively oxidize lignin in 3 h treatment (Figure S7). In addition, from the comparison between Figure 6a,b, it can be deduced that fewer intermediate products generate on this electrode. When a small amount of MAC AEs was added (Sb-SnO_2/MAC(0.01 g)), the pH and TDS variations were nearly identical to those of the 2D Ti/Sb-SnO_2 electrode. However, the UV-vis spectra change significantly versus time, where the absorbance increases at 290 nm. In addition, this phenomenon is more obvious when loading more MAC AEs (Sb-SnO_2/MAC(0.05 g) and Sb-SnO_2/MAC(0.10 g)), manifesting that MAC AEs could facilitate lignin depolymerization.

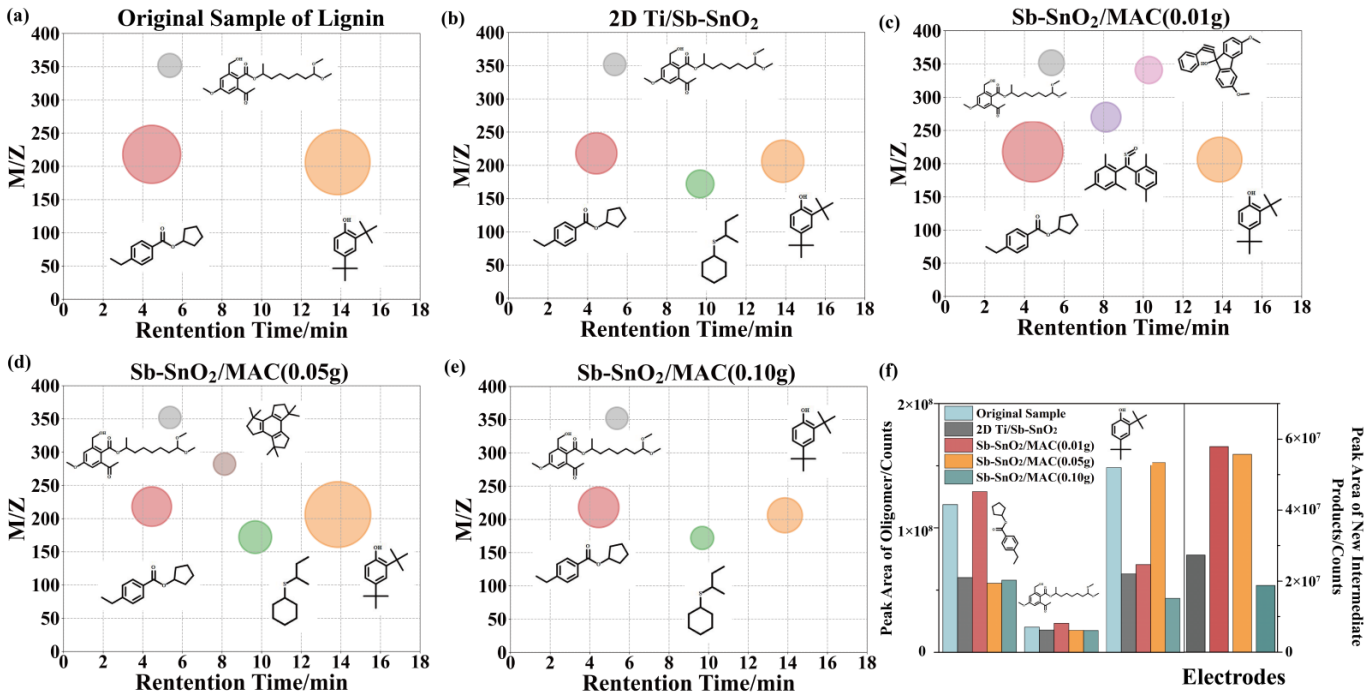

Figure 6. Lignin degradation results under current density of 20 mA·cm^{-2} (initial lignin concentration of 100 ppm, anode area of 9 cm^2, solution volume of 250 mL, supporting electrolyte of 125 ppm of Na_2SO_4, room temperature) before and after 3 h electrolysis (**a**–**e**) Bubble diagram of original lignin sample or intermediate products according to their GC peak area ((**a**) Original sample of lignin; (**b**) 2D Ti/Sb-SnO_2; (**c**) Sb-SnO_2/MAC(0.01 g); (**d**) Sb-SnO_2/MAC(0.05 g); (**e**) Sb-SnO_2/MAC(0.10 g); (**f**) Accumulative GC peak area columns of oligomers in original sample and degradation samples (left part) and new generated intermediate products after degradation (right part).

The efficiency and selectivity of the electrodes towards lignin and its intermediate products could be furtherly described by the GC-MS result of original lignin solution and treated samples. Lignin macromolecules are over the limit of GC-MS instrument, which could not be detected in the original lignin solution. However, three different oligomers (m/z: 206, m/z: 218, m/z: 352, respectively) are detected successfully (Figure 6a).

The variations of these three compounds are different depending on the electrode. In addition, a different type and amount of new intermediate products are generated by different electrodes (Figure 6b–e). The structures of these intermediate products derived from the reports given by the NIST database software could be used as reference. For example, although 2D Ti/Sb-SnO_2 electrode could not depolymerize lignin effectively (Figure S7), it is good at reducing the amount of the above three oligomers by ~50% in average. Sb-SnO_2/MAC(0.01 g) and Sb-SnO_2/MAC(0.05 g) accumulate some intermediate products (including new compounds as well as the original oligomers) originating from the depolymerization of lignin. However, Sb-SnO_2/MAC(0.10 g) not only depolymerize lignin more effectively (Figure S7) and reduce the original oligomers substantially, but also accumulates fewer new intermediate products. The superiority of Sb-SnO_2/MAC(0.10 g) is more obvious in degrading lignin thanks to the difficulty of treating polymer. As we can imagine, the previously demonstrated better electrochemical properties of this electrode (more active sites, larger surface area, faster charge transfer and mass transfer) may be more valuable in treating more complex and refractory wastewaters.

2.4. Cost-Effectiveness Estimation

The price of powdered AC used this study is only 2.3 ¥·kg^{-1}. The costs of other main agents (e.g., $FeSO_4 \cdot 7H_2O$ or $FeCl_3 \cdot 6H_2O$) used to fabricate MAC could also be negligible. The co-precipitation method to prepare MAC is simple and does not need high-temperature calcination procedures or device. Taking Sb-SnO_2/MAC(0.10 g) with geometric area of 1 m^2 for example, no more than 3 ¥ (loading 1 kg of MAC) of MAC and several magnets (e.g., ~200 ¥) are needed to enlarge electrode's electrochemical area by ~50% (according to Figure 2). The investment of 2D Ti/Sb-SnO_2 in this study is ~1500 ¥·m^{-2} (much lower than noble metal containing electrodes). However, the cost of the new strategy using MAC in this study is only ~27% of the potential additional investment of ~0.5 m^2 of 2D Ti/Sb-SnO_2 (~750 ¥). In addition, the operational cell voltage of galvanostatic electrolysis (or energy consumption) using Sb-SnO_2/MAC is ~10% lower than using 2D Ti/Sb-SnO_2, thanks to the well-conductive carbon-based MAC. Based on the above, loading MAC is cost-effective and advisable.

3. Experiments

3.1. Preparation of MAE

All reagents were analytical pure (Shanghai McLean Biochemical Co., Ltd., Shanghai, China). The ME substrate was a titanium plate with a thickness of 0.5 mm (Baosteel Group, Baoji, China). All solutions were prepared with ultra-pure water (Milli-Q water, Millipore, Milford, MA, USA). The MAC AEs were made using a chemical co-deposition method (details are placed in the Supporting Information Section), where the Fe_3O_4 grains were deposited on or into the active carbon (AC). The preparation of Ti/Sb-SnO_2 ME followed our previous report [22], using electrodeposition and a thermal oxidation method. The AEs were magnetically attracted and fixed on the ME surface by magnetic force. A permanent magnet (NdFeB) was attached to the back side of the ME with tape. The effects of AEs loading amount (0 g·cm^{-2}, 0.01 g·cm^{-2}, 0.05 g·cm^{-2}, and 0.1 g·cm^{-2}, respectively) on MAE performance were studied. Therefore, the assembled four electrodes were named 2D Ti/Sb-SnO_2, Sb-SnO_2/MAC(0.01 g), Sb-SnO_2/MAC(0.05 g), and Sb-SnO_2/MAC(0.10 g), respectively.

3.2. Material Characterizations

Scanning electron microscopy (SEM, JSM-6390A, JEOL, Tokyo, Japan) and X-ray diffraction (XRD, D/MAX-2200PC, Rigaku, Tokyo, Japan; Cu Kα, λ = 0.15406 nm) and a 3D digital microscope (VHX-7000, Keyence, Osaka Japan) were used to characterize the morphology, composition, and structure of ME, AEs, or MAE.

3.3. Electrochemical Characterizations

A typical three-electrode system was used to conduct the electrochemical characterization. The working electrode was the prepared MAE (exposed geometric area of 1 cm^2). The counter electrode was a 9 cm^2 copper plate. A saturated calomel electrode (SCE) served as the reference electrode. Narrow cyclic voltammetry (CV) ranging between 0–0.3 V (vs. SCE) was carried out in a 0.5 M Na_2SO_4 solution (with or without 2000 ppm of various organic pollutants). The scan rates used for narrow cyclic voltammetry (CV) were 0.005 $V{\cdot}s^{-1}$, 0.01 $V{\cdot}s^{-1}$, 0.02 $V{\cdot}s^{-1}$, 0.05 $V{\cdot}s^{-1}$, 0.1 $V{\cdot}s^{-1}$, and 0.2 $V{\cdot}s^{-1}$, respectively. The roughness factors of various electrodes can be calculated through fitting according to previous reports [13–15]. Linear scanning voltammetry (LSV) and the normal CV were performed between 0–2.5 V (vs. SCE) in the same solutions with a scan rate of 1 $mV{\cdot}s^{-1}$ and 10 $mV{\cdot}s^{-1}$, respectively. The electrochemical impedance spectroscopy (EIS) tests were conducted (vs. SCE) in the same solutions at equilibrium potentials of 0 V and 1.6 V (vs. SCE) with an amplitude of 5 mV, and a frequency range between 10^5 Hz to 0.1 Hz.

3.4. Pollutant Degradation

As model pollutants, sodium lignosulfonate (lignin, $C_{20}H_{24}Na_2O_{10}S_2$), phenol ($C_6H_5OH$), and the azo dye Red G (ARG, $C_{18}H_{13}N_3Na_2O_8S_2$) were used (structural formulas are shown in Scheme S2 of the Supporting Information). The wastewater (250 mL, 125 ppm Na_2SO_4 electrolyte) contained 200 ppm (for ARG) or 100 ppm (for phenol or lignin) of pollutants. Given that MAC would adsorb pollutants, each set of degradation experiments contained a 15-min resting period (adsorption process) prior to electrolysis to allow the pollutants to be adsorbed as possible. The studied anodic current densities were 2 $mA{\cdot}cm^{-2}$ and 20 $mA{\cdot}cm^{-2}$, respectively. The anode (effective electrode area of 9 cm^2) and cathode (copper sheet with the same size) were positioned parallel with a spacing of 15 mm. Room temperature served as the initial reaction temperature. In order to analyze the solution samples, a UV-Vis spectrophotometer (Agilent 8453, Santa Clara, CA, USA) and a multifunctional pH meter (LeiCi Group, Shanghai, China, including function of the total dissolved solids (TDS) determination) were used. The degradation intermediate products were identified by gas chromatography–mass spectrometry (GC–MS, Thermo Fisher, Waltham, MA, USA) using the NIST database.

4. Conclusions

The above results have demonstrated AC as a good alternative of metal oxide as a cost-effective AEs coating material of MAE.

1. MAC AEs improve the MAE's conductivity, increase electrochemical area, increase the number of active sites, facilitate charge transfer and mass transfer, and strengthen the electrode's direct oxidation (or DET) capability. These characteristics are more significant on the Sb-SnO_2/MAC(0.10 g).
2. More importantly, the loading amount of MAC AEs has a significant impact on various pollutant degradation rates and intermediate products accumulations. Sb-SnO_2/MAC(0.10 g) has the best pollutant degradation ability with the lowest amount of accumulated intermediate products.

This study has enriched the material system of MAE, completed the structure–activity relationship theory of MAE, and provided an additional theoretical basis and technical assistance to the application of EOWT towards actual organic wastewaters.

Supplementary Materials: The following supporting information can be downloaded at: https://www.mdpi.com/article/10.3390/catal13010007/s1, Text: Electrode preparation detail and voltammetric charge calculation; Scheme S1: Illustations of the C_{dl} calculation procedures; Scheme S2: Structrual formulas of the three pollutants used in this study; Figure S1: Narrow CV curves at different scan rates in 0.5 M Na_2SO_4 solution; Figure S2: Voltammetric charges obtained from the narrow CV curves (from 0 to 0.3 V (vs. SCE)) at different scan rates in 0.5 M Na_2SO_4 solution and 0.5 M Na_2SO_4 solution with 2000 ppm of ARG, lignin or phenol; Figure S3: LSV curves of the electrodes

(0 to 2.5 V (vs. SCE); scan rate: 0.001 $V \cdot s^{-1}$) in 0.5 M Na_2SO_4 solution and 0.5 M Na_2SO_4 solution with 2000 ppm of ARG, lignin or phenol; Figure S4: Normal CV curves of the electrodes (0–2.5 V (vs. SCE); scan rate: 0.01 $V \cdot s^{-1}$) in 0.5 M Na_2SO_4 solution and 0.5 M Na_2SO_4 solution with 2000 ppm of ARG, lignin or phenol; Figure S5: Other details of ARG degradation; Figure S6: Other details of phenol degradation; Figure S7: Other details of lignin degradation; References [9,23].

Author Contributions: Conceptualization, D.S.; methodology, D.S.; validation, F.Z. and D.S.; formal analysis, F.Z. and D.S.; investigation, F.Z.; resources, D.S., C.Y., H.X., J.Y., L.F., S.W., Y.L., X.J. and H.S.; writing—original draft preparation, F.Z.; writing—review and editing, D.S. and C.Y.; visualization, F.Z.; supervision, D.S., H.X. and H.S.; project administration, D.S.; funding acquisition, D.S. All authors have read and agreed to the published version of the manuscript.

Funding: This research was funded by the National Natural Science Foundation of China (21706153) and Natural Science Basic Research Program of Shaanxi Province (2018JQ2066, 2022JM-065).

Data Availability Statement: Not applicable.

Acknowledgments: The authors acknowledge the financial support from the National Natural Science Foundation of China and Natural Science Basic Research Program of Shaanxi Province.

Conflicts of Interest: The authors declare no conflict of interest.

References

1. Martínez-Huitle, C.A.; Rodrigo, M.A.; Sirés, I.; Scialdone, O. Single and Coupled Electrochemical Processes and Reactors for the Abatement of Organic Water Pollutants: A Critical Review. *Chem. Rev.* **2015**, *115*, 13362–13407. [CrossRef]
2. Radjenovic, J.; Duinslaeger, N.; Avval, S.S.; Chaplin, B.P. Facing the Challenge of Poly- and Perfluoroalkyl Substances in Water: Is Electrochemical Oxidation the Answer? *Environ. Sci. Technol.* **2020**, *54*, 14815–14829. [CrossRef]
3. Martínez-Huitle, C.A.; Panizza, M. Electrochemical oxidation of organic pollutants for wastewater treatment. *Curr. Opin. Electrochem.* **2018**, *11*, 62–71. [CrossRef]
4. Zheng, W.; Liu, Y.; Liu, W.; Ji, H.; Li, F.; Shen, C.; Fang, X.; Li, X.; Duan, X. A novel electrocatalytic filtration system with carbon nanotube supported nanoscale zerovalent copper toward ultrafast oxidation of organic pollutants. *Water Res.* **2021**, *194*, 116961. [CrossRef]
5. Panizza, M.; Cerisola, G. Direct and Mediated Anodic Oxidation of Organic Pollutants. *Chem. Rev.* **2009**, *109*, 6541–6569. [CrossRef]
6. Trellu, C.; Coetsier, C.; Rouch, J.-C.; Esmilaire, R.; Rivallin, M.; Cretin, M.; Causserand, C. Mineralization of organic pollutants by anodic oxidation using reactive electrochemical membrane synthesized from carbothermal reduction of TiO_2. *Water Res.* **2018**, *131*, 310–319. [CrossRef]
7. Ren, W.; Zhang, Q.; Cheng, C.; Miao, F.; Zhang, H.; Luo, X.; Wang, S.; Duan, X. Electro-Induced Carbon Nanotube Discrete Electrodes for Sustainable Persulfate Activation. *Environ. Sci. Technol.* **2022**, *56*, 14019–14029. [CrossRef]
8. Li, X.; Wu, Y.; Zhu, W.; Xue, F.; Qian, Y.; Wang, C. Enhanced electrochemical oxidation of synthetic dyeing wastewater using SnO_2-Sb-doped TiO_2-coated granular activated carbon electrodes with high hydroxyl radical yields. *Electrochim. Acta* **2016**, *220*, 276–284. [CrossRef]
9. Shao, D.; Yan, W.; Li, X.; Xu, H. Fe_3O_4/Sb–SnO_2 Granules Loaded on Ti/Sb–SnO_2 Electrode Shell by Magnetic Force: Good Recyclability and High Electro-oxidation Performance. *ACS Sustain. Chem. Eng.* **2015**, *3*, 1777–1785. [CrossRef]
10. Shao, D.; Zhang, X.; Lyu, W.; Zhang, Y.; Tan, G.; Xu, H.; Yan, W. Magnetic Assembled Anode Combining PbO_2 and Sb-SnO_2 Organically as An Effective and Sustainable Electrocatalyst for Wastewater Treatment with Adjustable Attribution and Construction. *ACS Appl. Mater. Interfaces* **2018**, *10*, 44385–44395. [CrossRef]
11. Zhang, X.; Shao, D.; Lyu, W.; Xu, H.; Yang, L.; Zhang, Y.; Wang, Z.; Liu, P.; Yan, W.; Tan, G. Design of magnetically assembled electrode (MAE) with Ti/PbO_2 and heterogeneous auxiliary electrodes (AEs): The functionality of AEs for efficient electrochemical oxidation. *Chem. Eng. J.* **2020**, *395*, 125145. [CrossRef]
12. Shao, D.; Zhang, X.; Wang, Z.; Zhang, Y.; Tan, G.; Yan, W. New architecture of a variable anode for full-time efficient electrochemical oxidation of organic wastewater with variable Cl− concentration. *Appl. Surf. Sci.* **2020**, *515*, 146003. [CrossRef]
13. Shao, D.; Zhang, Y.; Lyu, W.; Zhang, X.; Tan, G.; Xu, H.; Yan, W. A modular functionalized anode for efficient electrochemical oxidation of wastewater: Inseparable synergy between OER anode and its magnetic auxiliary electrodes. *J. Hazard. Mater.* **2020**, *390*, 122174. [CrossRef]
14. Zhang, Y.; Zhang, C.; Shao, D.; Xu, H.; Rao, Y.; Tan, G.; Yan, W. Magnetically assembled electrodes based on Pt, RuO_2-IrO_2-TiO_2 and Sb-SnO_2 for electrochemical oxidation of wastewater featured by fluctuant Cl- concentration. *J. Hazard. Mater.* **2022**, *421*, 126803. [CrossRef]
15. Shao, D.; Li, W.; Wang, Z.; Yang, C.; Xu, H.; Yan, W.; Yang, L.; Wang, G.; Yang, J.; Feng, L.; et al. Variable activity and selectivity for electrochemical oxidation wastewater treatment using a magnetically assembled electrode based on Ti/PbO_2 and carbon nanotubes. *Sep. Purif. Technol.* **2022**, *301*, 122008. [CrossRef]

16. Chaplin, B.P. Critical review of electrochemical advanced oxidation processes for water treatment applications. *Environ. Sci. Process. Impacts* **2014**, *16*, 1182–1203. [CrossRef]
17. Zhan, J.; Li, Z.; Yu, G.; Pan, X.; Wang, J.; Zhu, W.; Han, X.; Wang, Y. Enhanced treatment of pharmaceutical wastewater by combining three-dimensional electrochemical process with ozonation to in situ regenerate granular activated carbon particle electrodes. *Sep. Purif. Technol.* **2019**, *208*, 12–18. [CrossRef]
18. Giannakis, S.; Lin, K.-Y.A.; Ghanbari, F. A review of the recent advances on the treatment of industrial wastewaters by Sulfate Radical-based Advanced Oxidation Processes (SR-AOPs). *Chem. Eng. J.* **2021**, *406*, 127083. [CrossRef]
19. Du, X.; Oturan, M.A.; Zhou, M.; Belkessa, N.; Su, P.; Cai, J.; Trellu, C.; Mousset, E. Nanostructured electrodes for electrocatalytic advanced oxidation processes: From materials preparation to mechanisms understanding and wastewater treatment applications. *Appl. Catal. B Environ.* **2021**, *296*, 120332. [CrossRef]
20. Behling, R.; Valange, S.; Chatel, G. Heterogeneous catalytic oxidation for lignin valorization into valuable chemicals: What results? What limitations? What trends? *Green Chem.* **2016**, *18*, 1839–1854. [CrossRef]
21. Rafiee, M.; Alherech, M.; Karlen, S.D.; Stahl, S.S. Electrochemical Aminoxyl-Mediated Oxidation of Primary Alcohols in Lignin to Carboxylic Acids: Polymer Modification and Depolymerization. *J. Am. Chem. Soc.* **2019**, *141*, 15266–15276. [CrossRef] [PubMed]
22. Shao, D.; Yan, W.; Li, X.L.; Yang, H.H.; Xu, H. A Highly Stable Ti/TiHx/Sb-SnO_2 Anode: Preparation, Characterization and Application. *Ind. Eng. Chem. Res.* **2014**, *53*, 3898–3907. [CrossRef]
23. Montilla, F.; Morallón, E.; De Battisti, A.; Vázquez, J.L. Preparation and characterization of antimony-doped tin dioxide electrodes. Part 1. Electrochemical characterization. *J. Phys. Chem. B* **2004**, *108*, 5036–5043. [CrossRef]

Disclaimer/Publisher's Note: The statements, opinions and data contained in all publications are solely those of the individual author(s) and contributor(s) and not of MDPI and/or the editor(s). MDPI and/or the editor(s) disclaim responsibility for any injury to people or property resulting from any ideas, methods, instructions or products referred to in the content.